



Risk assessment of Triggered earthquake occurrences in the quarries Thuong Tan III, IV and adjacent area since the mining pit is impounded water

Trong Dinh Cao ^{1,*}, Nam Xuan Bui ², Tuan Anh Thai ¹, Hung Nam Pham ¹, Bach Xuan Mai ¹

¹ Institute of Geophysics, VAST, Vietnam

² Faculty of Mining, Hanoi University of Mining and Geology, Vietnam

ARTICLE INFO

Article history:

Received 15th June 2018

Accepted 20th Nov. 2018

Available online 31st Dec. 2018

Keywords:

Quarry;

Thuong Tan III, IV;

Natural earthquake;

Triggered earthquake;

Peak ground acceleration.

ABSTRACT

This paper presents the risk assessment of triggered earthquake in the quarries Thuong Tan III, IV after exploiting 100 m depth and impounding water for landscaped lake. Combination methods of gravity and electromagnetotelluric were used to estimate fault parameters, as well as fault segmentation method, was used to estimate the risk of the maximum magnitude of natural and triggered earthquake. Further, these fault parameters are considered as input information to computing the influence of the Thuong Tan III, IV reservoir impoundment by using the concept of fault stability Coulomb stress in order to assess the risk of triggered earthquake occurrence. The results show that: The quarries Thuong Tan III, IV are within the sphere of influence of second-order active fault Thien Tan - Binh Son. Triggered earthquake source has a length and width of 4.8 km and 1.8 km, respectively, with Strike angle = 140°, Dip angle = 80° and Rake angle = 180°. The maximum magnitude of natural earthquake in this source is 5.0 while that of the triggered earthquake is smaller than 3.2. The peak ground acceleration caused by triggered earthquake $M = 3.2$ in the lake Thuong Tan III, IV is 30.809 cm/s^2 , corresponding to the vibration of level V (MSK - 64, approximately 0.0308 g). With this vibration level, many people can feel the earthquake. Some unstable objects are overturned or moved. The Coulomb stress field at 2 km depth can reach the maximum value of 9.485 kPa. The region of positive Coulomb stress shows the influence of reservoir impoundment indicating the region of risk of triggered earthquakes occurrence.

Copyright © 2018 Hanoi University of Mining and Geology. All rights reserved.

1. Introduction

Triggering of earthquakes by filling of artificial water reservoirs is known for over six

*Corresponding author

E-mail: trongcd3284@gmail.com

decades, the first time pointed out by Carder (1945) at Lake Mead in the United States of America. The weight of water mass buckles the basement rock of lake bottom, causing subsidence (the subsidence of lake bottom can be up to 1.5÷2 m), which is the reason for triggering the reactivation of faults in the region, increasing the horizontal permeability, especially in the fracture zones. The increase of pore pressure in rock increases the infiltration, thus reducing the friction of existing conformities or failure surfaces. As a result, it decreases the firmness and changes the elastic coefficient of rock, causes the fluctuation of preceding tension force, leading to the displacement of rock mass towards the tectonic failure surface. It is unlikely that triggered earthquakes can occur in all reservoirs. As of today, over 90 sites have been globally identified where earthquakes have been triggered by filling of water reservoirs. Damaging earthquakes exceeding magnitude 6 occurred at Hsinfengkiang, China in 1962; Kariba, Zambia-Zimbabwe Border in 1963; Kremasta, Greece in 1966; and Koyna, India in 1967. The Koyna earthquake of M 6.3 that occurred on 10 December 1967 is so far the largest scientifically accepted triggered earthquake. There is an argument that the Sichuan, China, M 7.9 earthquake of 12 May 2008, which claimed over 80,000 human lives was triggered due to the filling of the nearby Zippingpu reservoir (Gupta and et al., 1972a, 1972b; Gupta, 2002; Gupta, 2011; Kalpna, Chander, 2000; Kalpna, Gupta, 2008; Kalpna, Hassoup, 2012; Kalpna and et al., 2016). It has also been proposed that flooding of a river near San Andreas Fault in California caused at least two ~ M 6 earthquakes (McGarr et al., 1997). Earthquakes occurrence around Aswan reservoir is also considered to be a case of reservoir triggered seismicity (RTS) where earthquakes continue to occur for the past ~ 35 years with the largest event of M 5.3 on 14 November 1981 (Telesca and et al., 2012; Telesca and et al., 2015). An earthquake of M 4.7 occurred at Song Tranh 2 (ST2), Vietnam on 15 November 2012 was assumed to be triggered by the reservoir impoundment as this region was otherwise regarded as largely aseismic (Trieu Dinh Cao and et al., 2014). A good account of triggered seismicity can be found in a review by Gupta

(2002). According to Professor Hash Gupta (Gupta, 2011), the percentage of reservoirs with depth of 90÷120 m in which triggered earthquake can occur is 6% (5/78 reservoirs); that with depth of 120÷150 m is 17% (5/29 reservoirs) and that with depth of 150÷250 m is 26% (5/19 reservoirs).

Triggered earthquakes have also occurred at some hydropower reservoirs in Vietnam, most notably in Hoa Binh, Song Tranh 2 and Son La (Xuyen Dinh Nguyen, 2004; Son Tu Le and et al., 2012). On May 23, 1989, an earthquake with M = 4.9 occurred in the Hoa Binh area after the hydropower reservoir was watered to the maximum elevation (90 m). Shortly after the Song Tranh hydropower reservoir was impounded (up to 96 m height), triggered earthquakes occurred, with the largest magnitude M = 4.7 on November 15, 2012. The strongest triggered earthquake at Son La hydropower reservoir has a magnitude of 4.3, recorded on July 19, 2014. The geological structures of Hoa Binh, Song Tranh 2 and Son La reservoirs are metamorphic rocks (including gneiss, metagabbro, metadiorite, meta-granodiorite, metaplagiogranite), granite, andesite or strongly cataclastic, fractured compact limestone.

The quarries Thuong Tan III, IV in Bac Tan Uyen district, Binh Duong province are currently exploited at -70 m. In the future, these quarries will be interconnectedly exploited to -100 m and converted into a landscaped lake. Does the water impoundment in a lake of such great depth cause triggered earthquake? That is the question that needs to be answered before the depth of exploitation and conversion of utility are approved. This paper presents the results of triggered earthquake risk assessment in the lake Thuong Tan III, IV.

In this paper, a comprehensive study is described which estimates fault parameters, the maximum magnitude of natural and triggered earthquake, peak ground acceleration of triggered earthquake and Coulomb stresses due to reservoir water load to see the effect of reservoir impoundment on the study region (Figure 1).

2. Determination of earthquake source parameters in the quarries Thuong Tan III, IV

Normally, the determination of earthquake



Figure 1. Diagram of the study profile of earthquake source structure based on gravity and electro-magnetotelluric data.

source (line source) is sequentially carried out as follows: 1/Detecting and classifying deep geological fault zones based on geological-geophysical data; 2/From the system of detected deep geological fault zones, classifying and identifying the faults that are likely to be active in the recent time; and 3/Determining earthquake source (line source) based on the analysis of earthquake activity characteristics of defined active faults.

2.1. Methodologies for determination of earthquake source parameters in the quarries Thuong Tan III, IV and adjacent area

2.1.1. Detection and classification of deep geological fault zones

Regional faults are detected on the basis of gravity and magnetic data according to some following indications and criteria (Trieu Dinh Cao and et al., 2014; Linh Van Đô and et al., 2008; Hung and et al., 2009):

1. Indications of faults based on magnetic, gravity anomaly maps (Figure 2 & 3) and anomaly field transformation map include: faults often related to extended gradient fields; the boundary between the two areas with different anomaly structure directions, or the intersection of anomalies with different structure directions; the displacement of extended linear anomalies and the appearance of flexures of contour line.

2. Using the calculation results of theoretical model in case of three-dimensional and two-dimensional problems when applying methods of

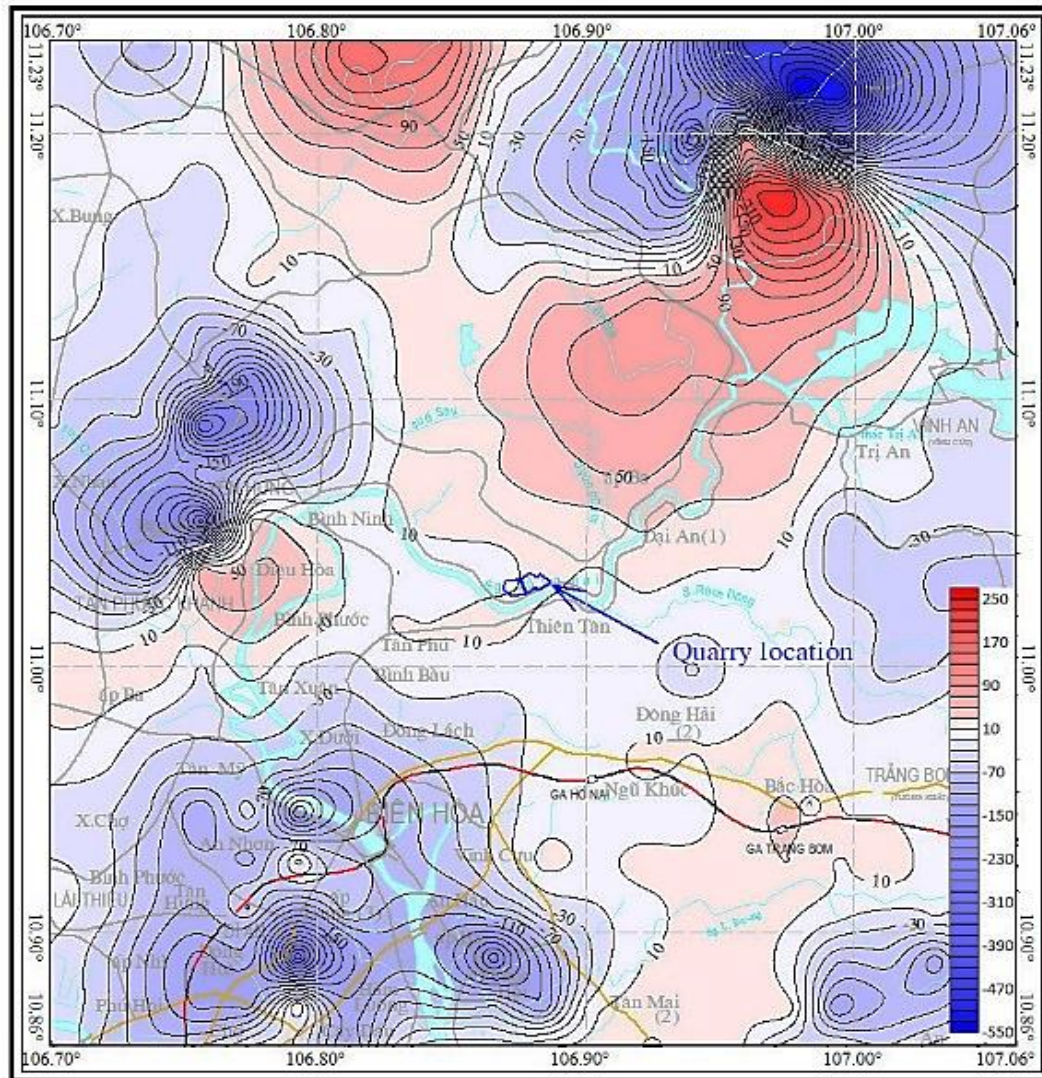


Figure 2. Magnetic anomaly map of the study region.

upward continuation, downward continuation, calculations of the gradient at different upward continuation heights, horizontal gradient, vertical gradient and normalized full gradient of gravity anomaly to each specific model. In case of upward continuation and calculation of horizontal gradient to different heights, the gravity anomaly field will reflect the characteristics of uplifts and depressions, which are the criteria for identifying fault existence. The calculation results of normalized full gradient of gravity anomaly give us the points which are specially related to the anomaly-causing blocks.

3. Calculation of horizontal gradient of gravity anomaly: In regard to geological research environment, when the boundary of density separation is vertical, the calculation result of

horizontal gravity gradient allows us to determine the extreme point (maximum or minimum) whose location often coincides with the interface of two different geological units. And that is often the spatial vertical boundary. If the interface is not vertical, the extremum of the horizontal gradient will be shifted towards the inclination; the positive extremum region is created just below the separation boundary and the negative one is on both sides.

4. Indications based on the calculation results of the linear normalized full vertical gradient are particular points when calculating the field reduction through geological objects. Particular points often appear in the object or coincide with the outer edges of geological objects causing an anomaly in the predetermined shape.

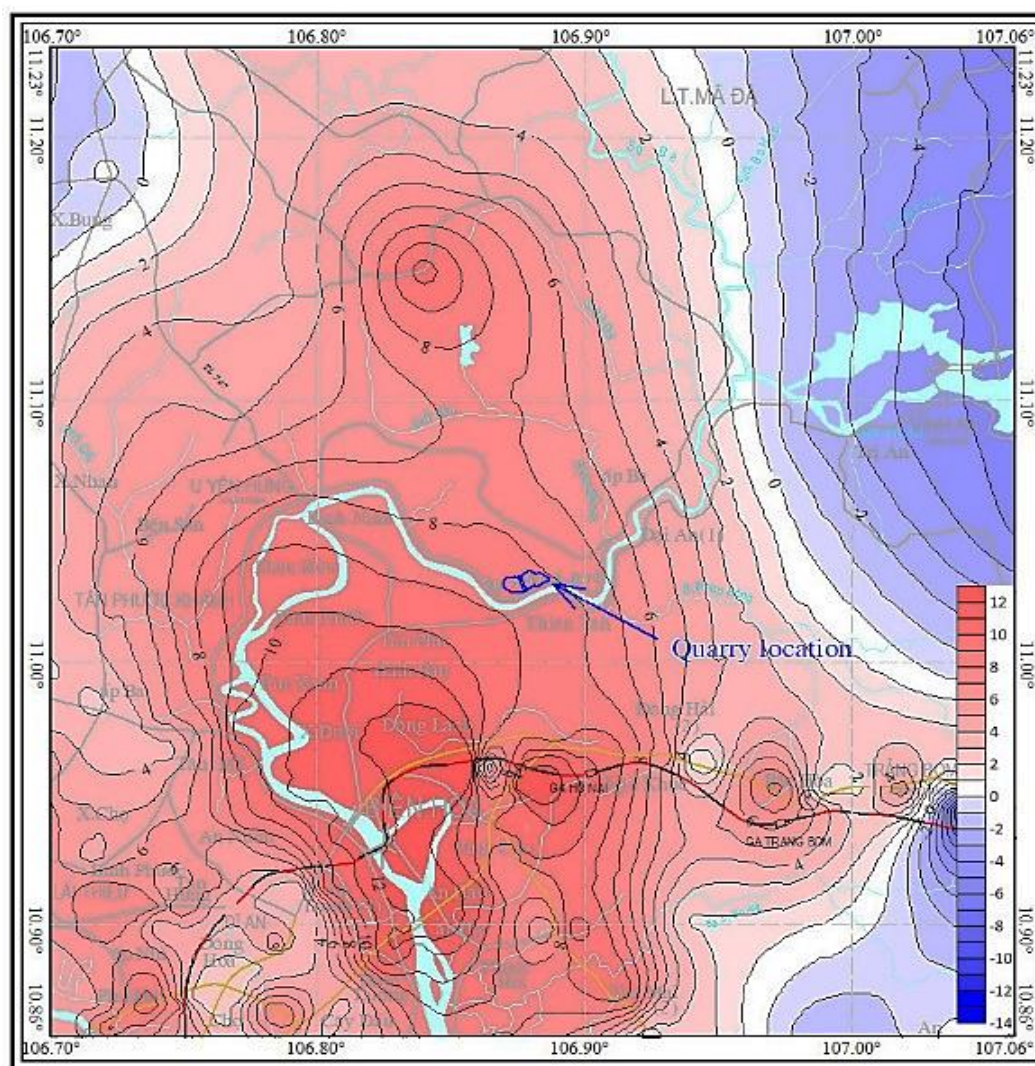


Figure 3. Bouguer gravity anomaly map of the study region.

2.1.2. Identification of active fault zones

The identification of active faults in the recent time is carried out by two approaches (Trieu Dinh Cao and et al., 2014; Linh Van Đô et al., 2008; Hung Cat Nguyen et al., 2009): direct and indirect (through the identification of boundary zone of the Earth's crust structure that is likely to be active in the recent time).

Direct indications include: 1/ Topographic scarps or a series of linear scarps, or extended straight valley profile or linear currents; 2/ Lineament continuously extending over a great length or profile of short lineaments (disrupted) crossing different structures; 3/ Changes of topographic and geomorphological elements; 4/ Manifestations of earthquake activity;

5/ Controlling valleys (grabens), Quaternary and recent sedimentary basins; 6/ Quaternary and recent volcanic; 7/ Source of hot water or deep-source mineral water; 8/ Phenomena of natural landslides, surface ruptures; and 9/ Measurement results (geodesy, repeated levelling, repeated gravity measurement, GPS, deformation measurement, Eman measurement).

The determination of active fault by indirect approach consists of two steps: 1/ Identifying and classifying (according to the secondary principle) the Earth's crust structure in the study area; and 2/ Comparing the movement characteristics (horizontal and vertical) of adjoining blocks to determine the activity characteristics of faults that play the role as the block boundary.

2.2. Data collection and analyses

In order to study the structural characteristics of earthquake source (natural earthquake and triggered earthquake) associated with the quarries Thuong Tan III, IV, the authors have conducted the gravity and electro-magnetotelluric measurements along the profile

perpendicular to the source of Thien Tan - Binh Son fault (Figure 1). In total, we have measured 20 electro-magnetotelluric points and 100 gravity points, the research ratio is 1/50,000. The analysis results of gravity and magnetotelluric data for studying fault structure are presented in Figures 4, 5.

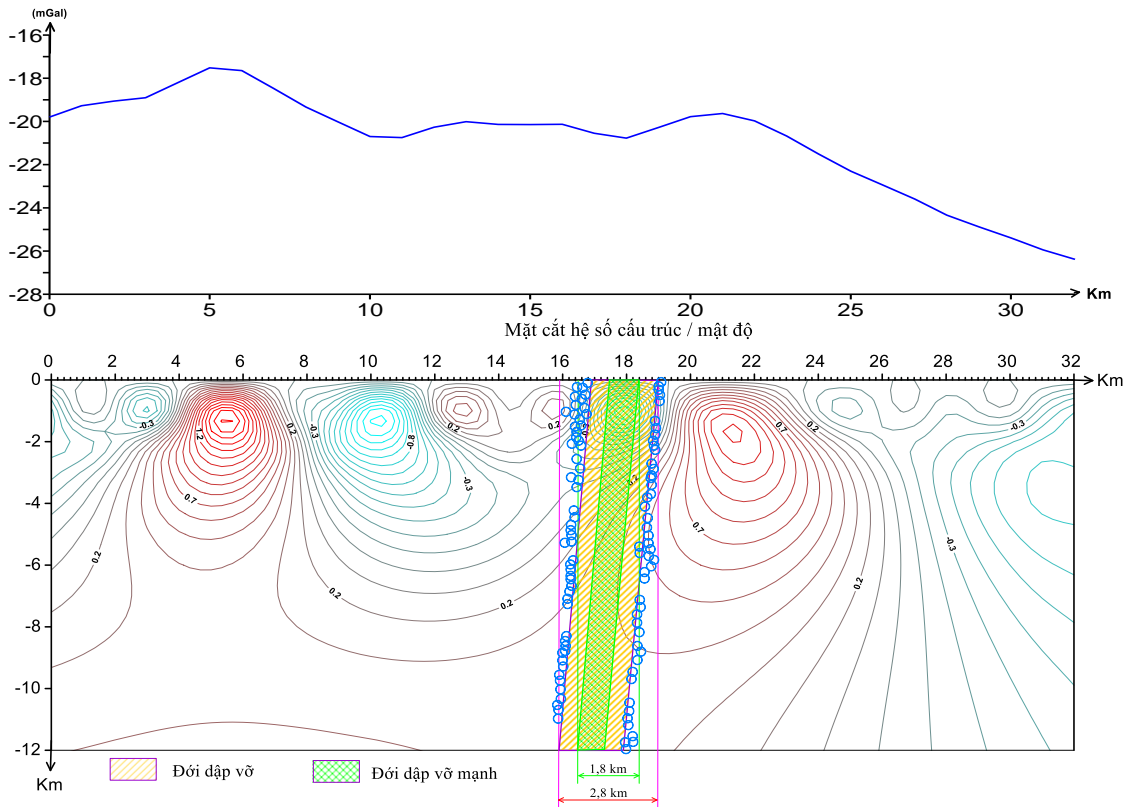


Figure 4. Cross section of components of gravity field transformation and earthquake source along the study profile.

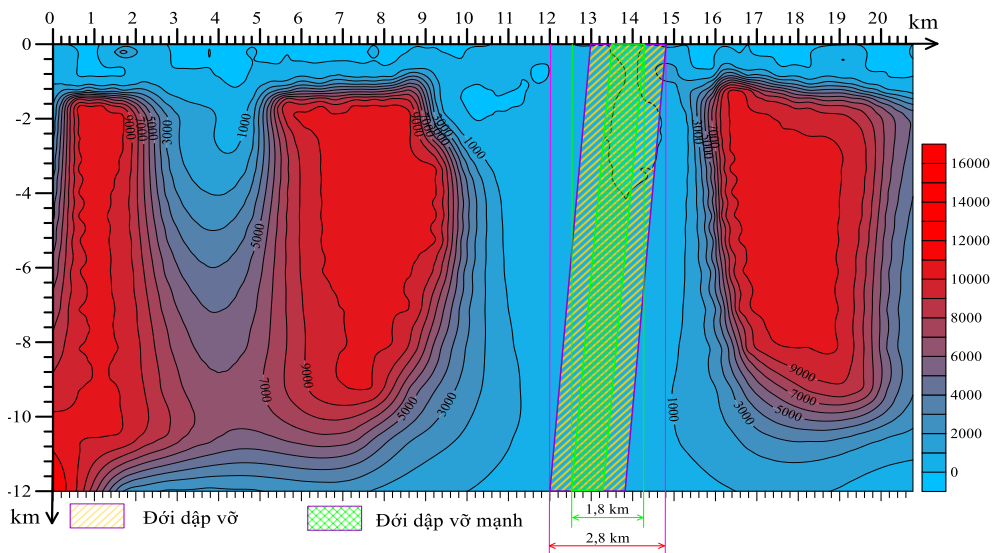


Figure 5. Cross section of resistance and earthquake source (according to cross section perpendicular to the source).

2.3. Structure of earthquake source in the quarries Thuong Tan III, IV

The active fault diagram in the quarries Thuong Tan III, IV and adjacent area is shown in Figure 6. The faults are classified into 2 orders: first order and second order. This is a local classification, the largest fault in the area is called the first order one, accompanied by the second order one. The faults of these two orders can possibly cause earthquakes with different magnitudes; the difference is usually set as 0.5 units by Vietnamese seismologists.

The first order faults in the study area include (Figure 6): Vam Co Dong River fault; Sai Gon River

fault (there are 2 accompanying faults: Dong Nai River and Thien Tan - Binh Son); Binh Long - Binh Chau fault and Loc Ninh - Ho Chi Minh sub-longitudinal fault. The quarries Thuong Tan III, IV and adjacent area are located in the region directly affected by Sai Gon River fault. Therefore, in this part we only go into the description of characteristics of Sai Gon River fault.

Sai Gon River fault divides Da Lat - Can Tho structure into two subregions (Linh Van Đô et al., 2008; Hung Cat Nguyen et al., 2009): Da Lat in the north and Can Tho in the south. The fault plays a role as the Cenozoic dynamic hinge between two different tectonic regimes: uplift, denudation during the Cenozoic in Da Lat subregion in the

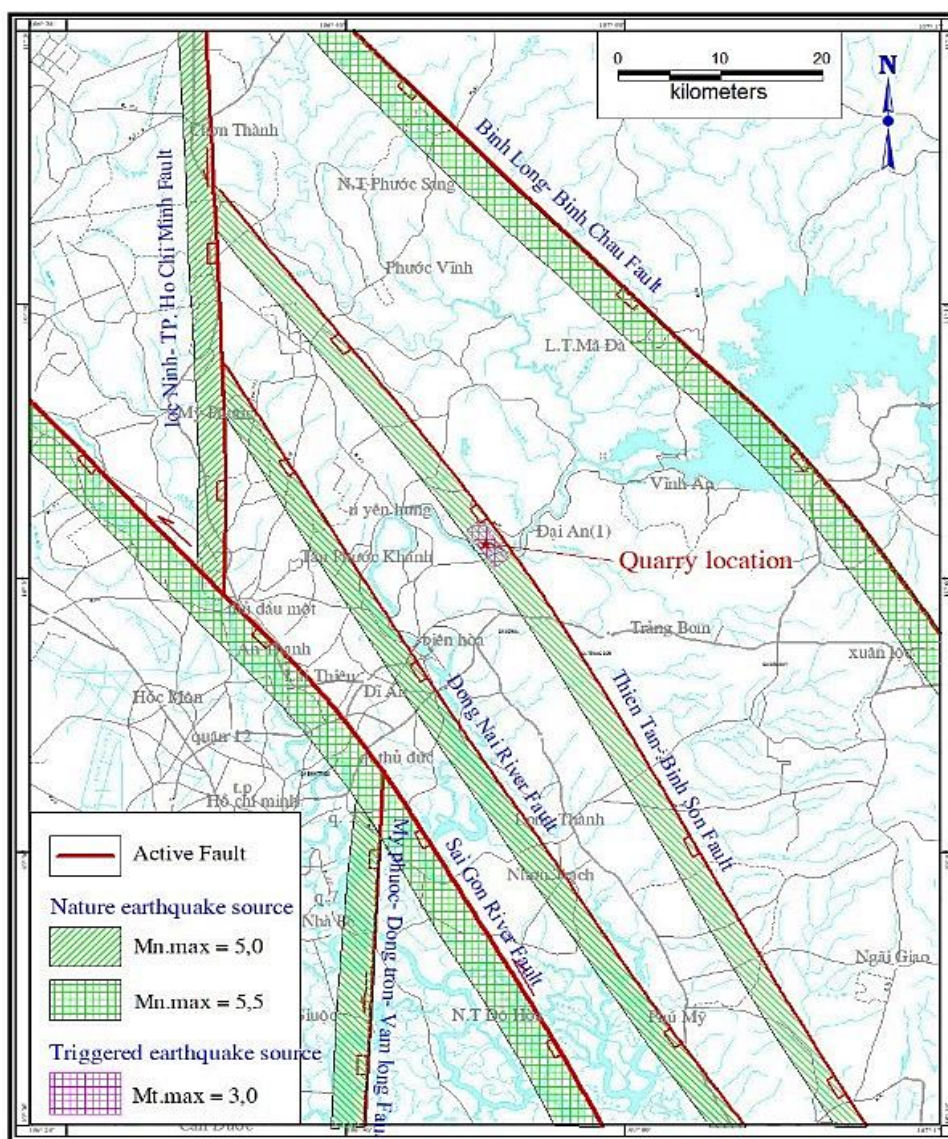


Figure 6. Distribution diagram of active faults in the quarries Thuong Tan III, IV and adjacent area.

northeast and subsidence, Cenozoic sedimentary fill, with the greatest thickness of 2100 m (Tra Cu basin) in Can Tho subregion. The results of fracture analysis show that the fault mainly dips towards the southeast with the average angle of $70\div 80^\circ$. The fault is relatively clear in gravity and magnetic data. The fault has the sphere of influence of about 30 km, nearly coincides with the photolineament and the DEM-Lineament reaches $200\div 300$ m/km². The depth of influence is through the crust. The dextral displacement amplitude of rivers based on the results of Landsat image analysis in 2002 is $500\div 2000$ m. The largest vertical displacement amplitude of the Cenozoic sedimentary basement is $330\div 446$ m (from Late Miocene).

The earthquake source related to the quarries Thuong Tan III, IV is presented in Figure 6. Based on the gravity, magnetotelluric methods and above-described fault segment, the earthquake source parameters are determined as follows:

- Natural earthquake source: length of 5 km; width of 2.8 km. The strongest observed earthquake has a magnitude of 4.5.

- Triggered earthquake source (the source area directly connected to the lake, which is the cluster of Thuong Tan III and Thuong Tan IV quarries after exploiting to 100m depth and impounding water): length of 4.8 km; width of 1.8 km. The strike of this source is 140° , the dip is 80° and the rake is 180° .

2.4. Assessment of maximum natural earthquake and triggered earthquake in the quarries Thuong Tan III, IV and adjacent area

Based on the assessment of strongest natural earthquake in the quarries Thuong Tan III, IV and adjacent area, some following conclusions can be drawn:

1. In the quarries Thuong Tan III, IV, and adjacent area, there are three earthquake sources: first-order earthquake source of Sai Gon River, second-order earthquake source of Dong Nai River and second-order earthquake source of Thien Tan - Binh Son (Table 1).

2. The strongest natural earthquake with a magnitude of 5.5 can occur in the source of Sai Gon River. Meanwhile, the maximum natural earthquake that can occur in the sources of Dong

Nai River and Thien Tan - Binh Son only has a magnitude of 5.0.

3. The quarries Thuong Tan III, IV are located within the earthquake source of Thien Tan - Binh Son, so they are affected by earthquake activity of this source. The strongest earthquake that can occur in these quarries has a magnitude of 5.0.

4. The triggered earthquake source in lake Thuong Tan III, IV has a length of 4.8 km and a width of 1.8 km. The maximum magnitude of triggered earthquake can only be less than 3.2.

5. The peak ground acceleration caused by triggered earthquake $M = 3.2$ in the lake Thuong Tan III, IV is 30.809 cm/s², corresponding to the vibration of level V (MSK-64, approximately 0.0308g). With this vibration level, many people can feel the earthquake. Some unstable objects are overturned or moved. The vibration is like being caused by heavy objects falling in the house.

3. Calculation of coulomb stress caused by reservoir load in the Thuong Tan III, IV region

According to Bell and Nur (Bell and Nur, 1978), the change of Coulomb stress (ΔS) caused by water impoundment in the reservoir is determined as follows: $\Delta S = \Delta\tau - \mu(\Delta\sigma_n - \Delta P)$, where $\Delta\tau$ and $\Delta\sigma_n$ correspond to the changes of shear stress and normal stress which are caused by the reservoir capacity on the fault surface, ΔP is the change of pore pressure, and μ is the coefficient of friction. The increase of $\Delta\tau$ and the decrease of $\Delta\sigma_n$ mean that ΔS has a positive value, which will stimulate the fault activity and vice versa. The role of pore pressure always promotes the fault activity due to the lubrication on the fault surface and the decrease of normal stress $\Delta\tau$.

Based on the above theoretical basis, the research team calculated stress components and Coulomb stress caused by the reservoir capacity on the study area. The reservoir is subdivided into small blocks, the parameters of length, width, and depth at each block are determined. The fault parameters consisting of the strike, dip, and rake are included to calculate the change of stress field. In the study area, Thien Tan - Binh Son fault near the lake is considered active and the parameters of this fault (strike = 140° , dip = 80° , rake = 180°) are included in the calculation. Other parameters are included in the calculation as follows:

the study area is gridded into $0.0018^{\circ} \times 0.0018^{\circ}$; Poisson's ratio $\nu = 0.25$; Skempton's coefficient $B = 0.7$; coefficient of friction $\mu = 0.65$.

From the above input parameters, the calculations are based on the scenario in which the reservoir is fully impounded and the tectonic stress field in the area is unchanged at the calculation time. Components of Coulomb stress field are calculated at the depths of 2 km, 4 km, 6 km, and 8 km, respectively. The calculation results show that the areas with a positive value of Coulomb stress ΔS are at risk of triggered earthquake occurrence when the reservoir is fully impounded. On this basis, it is possible to

delineate the areas at risk of reservoir-triggered earthquake

The detailed calculation results of maximum stress increase at 100m depth are presented in Figure 7 (a, b, c, d) and Table 2.

- The Coulomb stress field at 2 km depth can reach the maximum value of 9.485 kPa (Figure 7a); The Coulomb stress field at 4 km depth can reach the maximum value of 3.003 kPa (Figure 7b); The Coulomb stress field at 6 km depth can reach the maximum value of 1.398 kPa (Figure 7c); The Coulomb stress field at 8 km depth can reach the maximum value of 0.801 kPa (Figure 7d).

Table 1. Faults directly impacting on deformation and earthquake in the study area (Figure 6).

No.	Fault	Length (km)	Extending direction	Order	DD/DA	Slip in N2 - Q	M	SA	SI	DI
1	Sai Gon River	20, 36, 52	NW - SE	I (II)	SW/75	Dextral strike-slip - normal	5.5	22	30	30
2	Dong Nai River	75	NW - SE	II (III)	SW/85	Dextral strike-slip - normal	4.5	10	10	12
3	Thien Tan - Binh Son	80	NW - SE	II (III)	SW/75	Dextral strike-slip - normal	4.5	10	10	12

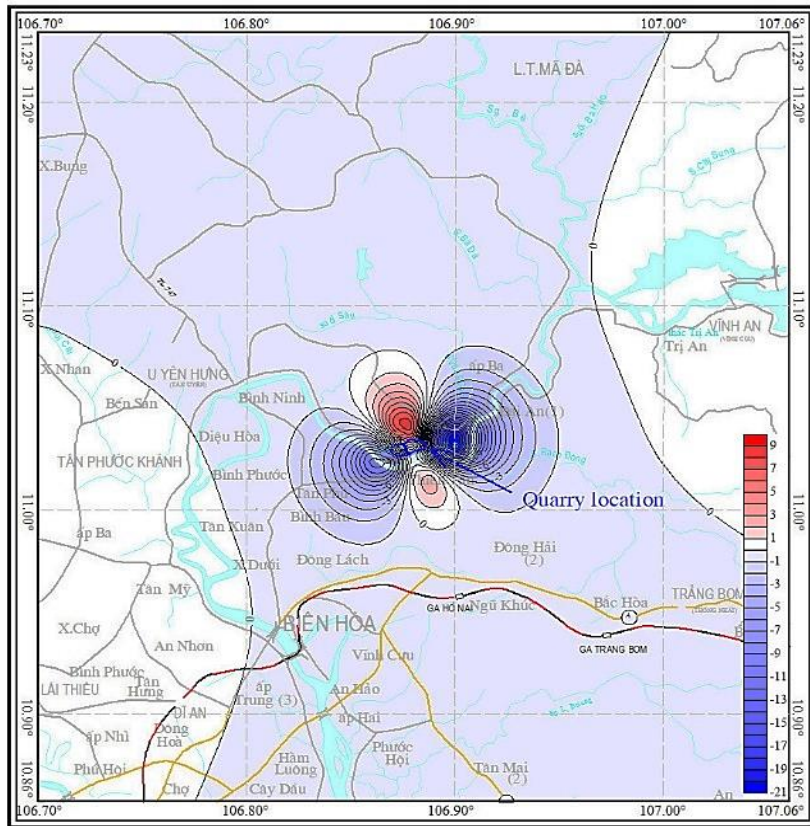


Figure 7a. Coulomb stress caused by reservoir capacity at 2km depth.

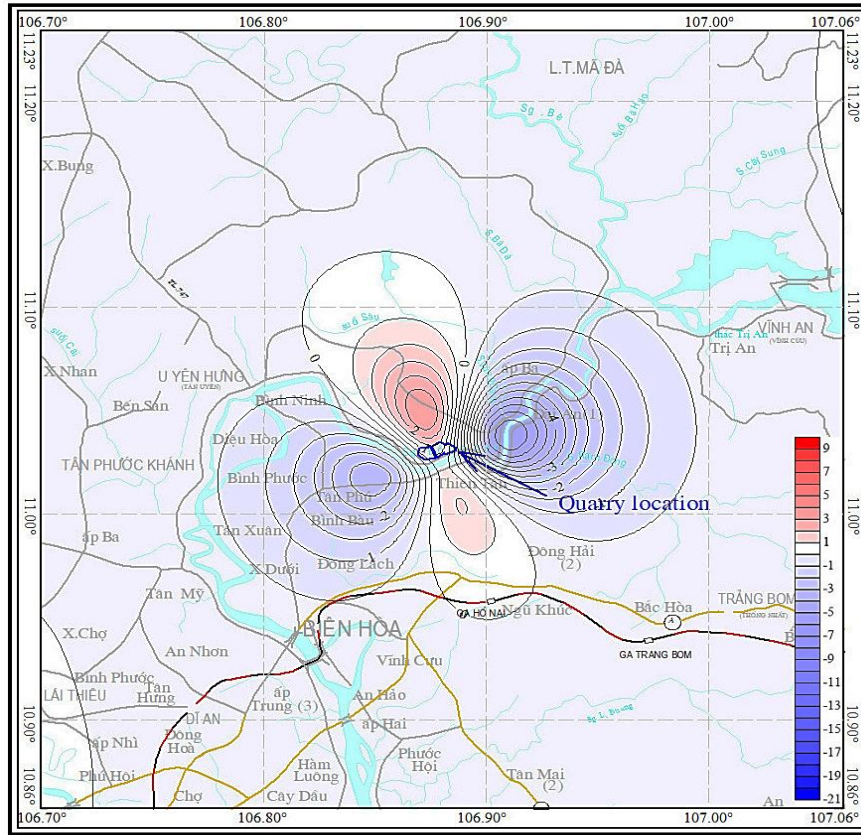


Figure 7b. Coulomb stress caused by reservoir capacity at 4km depth.

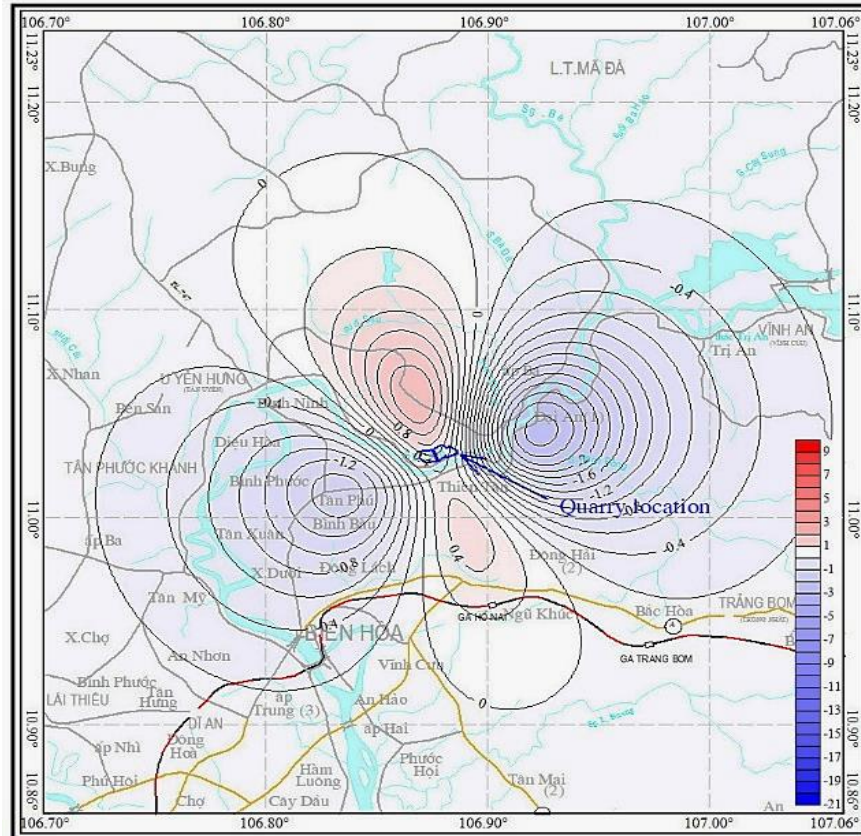


Figure 7c. Coulomb stress caused by reservoir capacity at 6km depth.

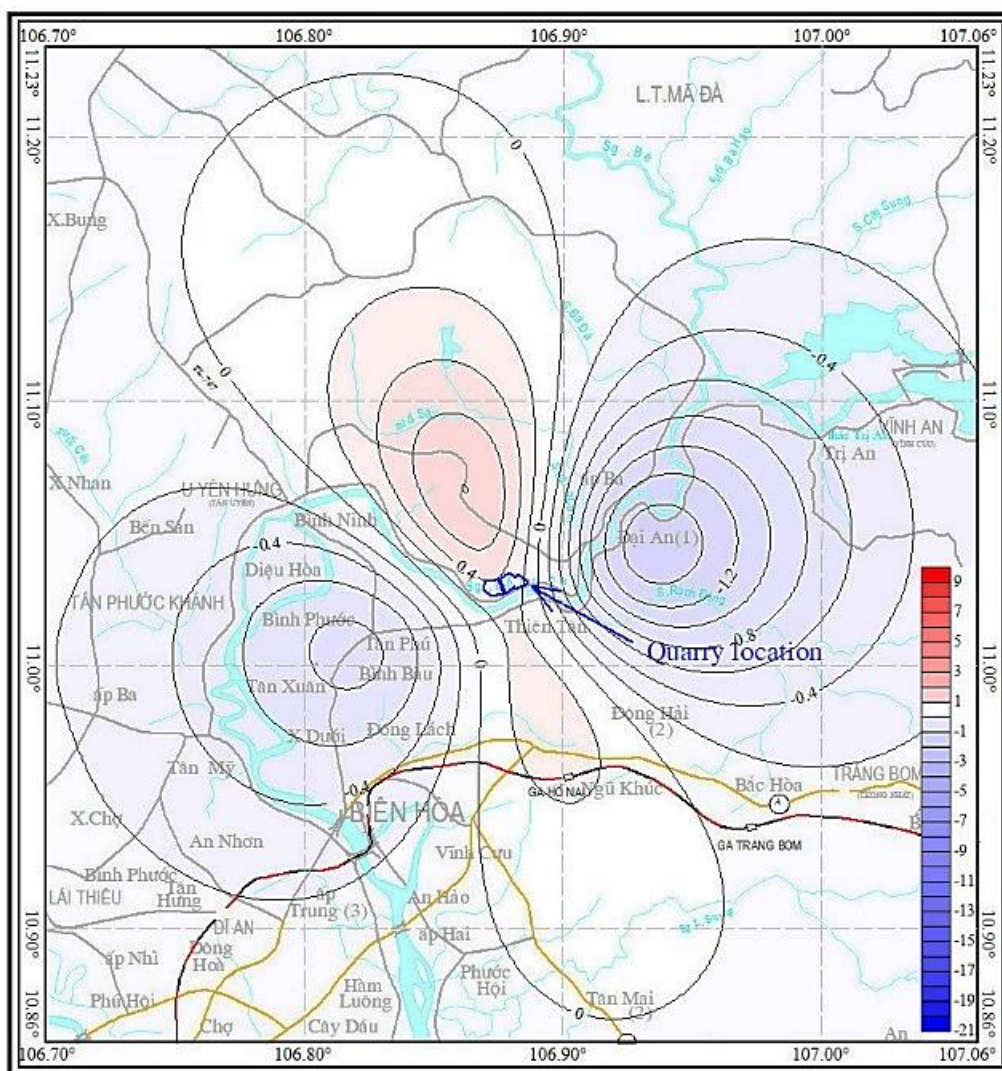


Figure 7d. Coulomb stress caused by reservoir capacity at 8km depth.

Table 2. Maximum value of Coulomb stress caused by reservoir load at 100m depth.

Scenario of reservoir depth	The maximum value of Coulomb stress at different depths (kPa)			
	2 km	4 km	6 km	8 km
100 m	9.485	3.003	1.398	0.801

4. Conclusion

Based on the research results, some following conclusions can be drawn:

1. The quarries Thuong Tan III, IV are located within the Dau Tieng - Ba Ria massif, extend in the NW - SE direction and bounded on both sides by two NW - SE faults, namely Sai Gon River fault in the southwest and Binh Long - Binh Chau fault in the northeast.

2. Thien Tan - Binh Son fault is essentially an accompanying branch of the main Sai Gon River

fault. The fault is assessed as active in Late Miocene - Pleistocene, in Holocene and recent times, according to the Eman measurement data. The quarries Thuong Tan III, IV are located within the sphere of influence of second-order active fault Thien Tan - Binh Son.

3. The earthquake source in lake Thuong Tan III, IV has a length of 4.8 km and a width of 1.8 km. The maximum magnitude of natural earthquake in this source is 5.0 and that of the triggered earthquake is smaller than 3.2.

4. Modeling of stresses due to the water load of the Thuong Tan III, IV reservoir indicates that the Coulomb stress field will reach the value of 9.485 kPa, the regions with positive Coulomb stress ΔS are at risk of triggered earthquake occurrence. Compared to the breaking stress of rock in the earthquake, the calculation value is very small, only about 1%. It plays a role as the promoting mechanism and only makes sense when natural stress reaches its limit.

5. The peak ground acceleration caused by triggered earthquake $M = 3.2$ in the lake Thuong Tan III, IV is 30.809 cm/s², corresponding to the vibration of level V (MSK-64, approximately 0.0308 g). With this vibration level, many people can feel the earthquake. Some unstable objects are overturned or moved.

References

- Bell, M. L., Nur, A., 1978. Strength changes due to reservoir induced pore pressure and stresses and application to Lake Oroville. *J. Geophys. Res.* 83, 4469 - 4483.
- Cao Đình Triêu, Cao Đình Trong, Lê Văn Dũng, Thái Tuấn Anh, and Đinh Quốc Văn, and Hà Vinh Long, 2014. Triggered earthquake study in Tranh River no. 2 (Vietnam). *Hydropower Reservoir. Journal Geological Society of India* 84, 319 - 325.
- Cao Đình Trong, Nguyễn Anh Dũng, Thái Tuấn Anh, Cao Đình Triêu, 2016. Characteristics of triggered earthquake activity in Da River cascade hydropower plant. *Journal of Geology, Series A, No. 361-362* (11-12). 80-93 (in Vietnamese).
- Cat Nguyễn Hùng (chief author) et al., 2009. Earthquake microzoning in Ho Chi Minh City. *Final project report (Stored in South-Vietnam Geological Mapping Division. Institute of Geophysics)*. 360p (in Vietnamese).
- Đo Văn Linh, Vũ Đình Chinh, La Thị Chích, 2008. The Pliocen - Quaternary tectonic stress field in South Vietnam and its influence on deformation of Precenozoic basement of Cuu Long basin. *The 2-nd International Scientific Conference "Fracture Basement Reservoir"* Petrovietnam. 9-10/ September 2008, Vung Tau-Viet Nam. 51 - 62.
- Gupta, H. K., 2002. Reservoir induced earthquakes. *Developments in Geotechnical Engineering. Elsevier, Netherlands*. 64.
- Gupta, H. K., 2011. *Encyclopedia of Earth Sciences Series. Springer, Netherlands*.
- Gupta, H. K., Rastogi, B. K., Narain, H., 1972a. Common features of the reservoir associated seismic activities. *Bull. Seismol. Soc. Am.* 62. 481 - 492.
- Gupta, H. K., Rastogi, B. K., Narain, H., 1972b. Some discriminatory characteristics of earthquakes near the Kariba, Kremasta and Koyna artificial lakes. *Bull. Seismol. Soc. Am.* 62. 493 - 507.
- Kalpna, Chander, R., 2000. Green's function based stress diffusion solution in the porous elastic half space for time varying finite reservoir loads. *Physics of the Earth and Planetary Interiors* 120. 93 - 101.
- Kalpna, Hassoup, A., 2012. Role of fluids in the earthquake occurrence around Aswan reservoir, Egypt. *Journal of Geophysical Research* 117. B02303.
- Kalpna, Pravin K. Gupta, 2008. An integral equation algorithm for 3-D simulation of pore pressure in a porous elastic medium with heterogeneities. *Geophysical Journal International*. 175.
- Kalpna, Tuấn, T.A., and N. Purnachandra Rao, 2016. Rapid and Delayed Earthquake Triggering by the Song Tranh 2 Reservoir, Vietnam. *Bull Seismol. Soc. Am.*, 106 (5).
- Le Tu Sơn (chief author), 2012. Study on triggered earthquake forecasting in Son La hydropower reservoir. *Final report of state-level independent project, code DTDL.2009T/09, stored in Institute of Geophysics*. 271 (in Vietnamese).
- Nguyễn Đình Xuyên (chief author), 2004. Tectonic geology and strong earthquake-generating areas in the Vietnam's territory. *Stored in Institute of Geophysics*. 330 (in Vietnamese).

Telesca L., ElShafey Fat ElBary R., Amin Mohamed A. E., ElGabry M., 2012 Analysis of the cross-correlation between seismicity and water level in the Aswan area (Egypt) from 1982 to 2010. *Nat Hazards Earth Syst Sci* 12. 2203 - 2207.

Telesca L., Giocoli A., Lapenna V., Stabile T. A., 2015 Robust identification of periodic behavior in the time dynamics of short seismic series: the case of seismicity induced by

Pertusillo Lake. *southern Italy. Stoch Environ Res Risk Assess* 29. 1437 - 1446.

Thai Anh Tuan, N. Purnachandra Rao-, Kalpna Gahalaut, Cao Dinh Trong, Le Van Dung, Cao Chien, K. Mallika, 2017. Evidence that earthquakes have been triggered by reservoir in the Song Tranh 2 region. Vietnam. *Journal of Seismology* 21 (5). 1131 - 1143.